Load reduction using pressure difference on airfoil for control of trailing edge flaps

Gaunaa, Mac; Andersen, Peter Bjørn

Published in:
EWEC 2009 Proceedings online

Publication date:
2009

Document Version
Publisher's PDF, also known as Version of record

Load Reduction Using Pressure Difference on Airfoil for Control of Trailing Edge Flaps

Mac Gaunaa
Risø DTU
macg@risoe.dtu.dk

Peter Bjørn Andersen
Risø DTU
pbja@risoe.dtu.dk

Abstract:

This work investigates the fatigue load reduction potential of using unsteady measurements of pressure differences over the pressure and suction sides of an airfoil to control a Trailing Edge (TE) flap. Analysis using unsteady thin airfoil potential flow theory shows that a fairly good estimation of the unsteady lift of an airfoil equipped with a TE flap is possible using a measurement of the pressure difference at only one single chordwise position. Theory furthermore predicts a very accurate prediction of unsteady lift using measurement of the unsteady pressure differences at two different chordwise positions. These insights were used to develop two simple TE control algorithms based on pressure measurements on an airfoil. Simulations in a 2D aeroelastic simulation tool showed that the control algorithm based on one pressure difference measurement resulted in a good load reduction potential whereas the TE control based on the finer estimation of the unsteady loads turned out to be aeroelastically unstable due to coupling with the structural torsional degree of freedom.

Keywords: Smart Rotors, Trailing Edge Flaps, Load Alleviation.

1 Introduction

The main driver of fatigue loads on wind turbines is the fluctuating nature of the aerodynamic loads due to turbulence, shear, gusts, operation in yaw, tower shadow, etc. Alleviating these loads can reduce materials consumption or increase the lifetime of the turbine components.

Investigations of using the pitch system for alleviating these loads [1,2] have shown promising results, but recent studies [3,4,5-12] have shown that even higher load reductions may be possible by employing local aerodynamic control, such as for instance trailing edge flaps [3, 5-12]. Furthermore, as wind turbines increase in size and get more flexible, there is an increased need for locally distributed control surfaces.

By enabling the trailing edge to move independently and quickly at different radial positions along the blade, local fluctuations in the aerodynamic forces due to changes in the relative flow magnitude and direction can be compensated for by deformation of the airfoil geometry.

At Risø DTU - National Laboratory for Sustainable Energy in Denmark, continuous research for many aspects of Adaptive Trailing Edge Flaps (ATEF) for wind turbine applications have been carried out during the last five years [5-12]. Due to performance and noise issues the work from Risø has focused on a special type of trailing edge deformation where the discontinuity on the airfoil surface associated with rigid trailing edge flaps are avoided. In [7] a CFD study of different trailing edge deformation mode shapes was investigated, and it was concluded that a 10% deformable trailing edge corresponded well to the requirements of applications on the outer sectios on an PRVS wind turbine. A representation of a generic ATEF system is illustrated in Figure 1.

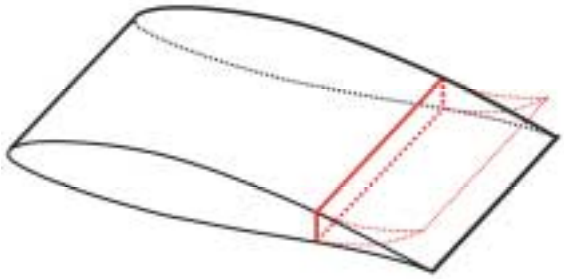

Figure 1: Conceptual design layout of a airfoil section with a deformable trailing edge flap. From [13]. Used with permission.

At Risø DTU an unsteady 2D potential-flow model for the aerodynamic forces of a thin airfoil undergoing a general deformation of the camberline was developed [9]. This model employs the use of indicial function response functions and can be used in both eigenvalue-based and time simulation-based algorithms. Due the use of indicial response functions, the computational requirements for time simulation is very low, in the order of a classic flat plate potential flow time series also employing the computationally efficient indicial function response method. Apart from the usually used integral quantities lift and moment, the model [9] provides also unsteady drag, generalized forces corresponding to the deformations of the camber-line and local unsteady pressure differences over the airfoil.

An extension of the potential flow model to take into account also viscous effects was described in [5]. The unsteady characteristics in attached flow stems from the potential flow model [9]. Recent work using this model in the 3D aeroelastic computational code HAWC2 [16] has showed load reduction potentials of up to 40% of blade root moment in the flapwise direction [10].

Analysis of the implications on the aeroelastic stability of adding a TE control system was investigated in [14,15] in a 2D setting. These investigations showed that the stability limits in general are lowered when using trailing edge flaps for load alleviation compared to an uncontrolled airfoil section. However, the changes in stability limits were found to be highly dependent on the control method and parameters. Stability investigations were performed for the control algorithms suggested by Buhl *et.al.*[8]. For the control based on pitot tube measurements the drop in instability velocity is generally much less than the corresponding drop using a control based on out-of-rotorplane deflections, which showed to be rather unstable. A recent paper [13] investigated the aeroservoelastic stability on a 3D model of a wind-turbine, which confirmed that the indications obtained using the much simpler and computationally efficient 2D models were qualitatively correct.

Even though much work has been carried out (load reduction potential, possible control strategies, closed loop testing in tunnel), there are still many unresolved issues that have to be tackled before the trailing edge flap concept can be effectively used on MW size wind turbines. Many of these issues are linked to the sensoring of the state of the wind turbine, on which the TE flap is to act. Previous works have used measurements of quantities such as for instance out-of-rotorplane deformations and angles of attack (using a pitot tube) on the rotors. Many of these data are hard to measure and use due to noise issues, time delay and other issues linked to measuring the quantities, as shown in [11]. Therefore, the present paper undertakes a first investigation of the load reduction potential using the difference pressure measured over the airfoil to control the trailing-edge flap, as this difference pressure is relatively straightforward to measure on a real wind turbine. In order to simplify matters, a 2D model, such as first used by Buhl *et.al.* [8], is employed for the present analysis. Earlier studies have shown that the load reduction potential and stability behavior revealed in the simple 2D models is a good indicator of the behavior in the physically more correct, but computationally much heavier 3D aeroelastic models.

2 Theory & Method

An underlying assumption in the two different control schemes considered in [8] is that controlling the trailing edge angle with the aim of keeping the lift constant is beneficial for a wind turbine. The first of the control algorithms seeks to minimize the fluctuations in the the out-of-rotorplane deformation of the airfoil section using a simple PID control algorithm. Keeping the out of rotorplane coordinate constant corresponds to keeping the lift constant despite the turbulent inflow. The second control algorithm presented in [8] is based on measuring the direction of the flow relative to the airfoil section using a pitot tube, and then using a quasi-steady assumption for the aerodynamic forces, prescribing the position of the trailing edge such that the quasi-steady lift is kept constant. In [8] it was shown that the load reduction capabilities of the proposed sensor/algorithm combinations were very efficient in reducing fatigue loads. In real life it may, however, be rather difficult to measure the actual out of plane deformation of a wind turbine

accurately and with a high temporal resolution. Likewise, estimating the angle of attack of the flow undisturbed by the wing requires some processing, which may introduce a time lag which has a very big negative influence on the obtainable load reduction [8]. The pitot-tube solution may also be fragile. Usually pitot-tubes are used in applications where they are easily and often checked. This will not be the case for applications on wind turbines. Therefore, other ways of sensing the state of the wind, loads or wing is still interesting in this field.

In this section, a model for estimation of the unsteady lift on an airfoil with a TE flap (rigid or continuously deforming) in attached flow conditions based on measurements of the pressure differences over the airfoil in one or two chordwise positions will be described. Thereafter these models will be used to construct simple PI control algorithms for the TE flap based on the estimation of the lift from the pressure measurements.

The benefit of such an approach would be a simpler, more robust and probably cheaper sensoring method than the pitot tube solution.

2.1 Estimation of unsteady lift using pressure difference measurements

One of the most widely used simple models for unsteady airfoil performance is thin airfoil theory. The basic assumptions in thin airfoil theory are that effects connected to airfoil thickness and viscosity[1] can be neglected. Thin airfoil theory is based on potential flow, and results in a linear system. The assumptions under which thin airfoil theory is derived corresponds to fully attached flow, so it is a fair representation of the local aerodynamic behavior on the outer sections of a Pitch Regulated Variable Speed (PRVS) wind turbine. Since smart rotor aerodynamic control devices such as deformable trailing edge geometry (TE flaps) needs to be located in this region of the blades to be most effective for load reduction, thin airfoil theory is an obvious choice for unsteady aerodynamic modeling in this case. Despite the crude assumptions made in this theory, comparison with more complex models (see for instance [7,17]) show that the simple model represent the main characteristics of for instance the much more complex CFD computations.

Gaunaa [9] previously derived a model applicable for the case of airfoils with generally deformable chords. Apart from the integral forces on the airfoil, the model also provides the generalized forces for the deformation modes and the unsteady pressure difference over the airfoil. Since the pressure difference over the airfoil is fairly straightforward to measure on a real wing, and the unsteady pressure difference on over the wing is closely related to the integral lift force, we will now outline two algorithms, derived from the potential flow model in [9], for determination of the unsteady lift based on either one or two pressure difference measurements.

Analysis of the unsteady thin-airfoil potential flow solution in [9], neglecting the effect from the motion of the airfoil in the *x*-direction[2] (corresponding roughly to the in-rotorplane motion), reveals the following general linear relations for the integral lift and pressure difference between the pressure and suction sides on an airfoil:

$$\frac{L}{0.5\rho V^2 c} = k_C \alpha_{C,eff} + k_{\dot{\alpha}} \frac{\dot{\alpha} c}{V} + k_L(\ddot{y}, \ddot{\alpha}, \dot{\beta}, \ddot{\beta}) \quad (1)$$

$$\frac{\Delta p(x)}{0.5\rho V^2} = g_C(x)\alpha_{C,eff} + g_{\dot{\alpha}}(x)\frac{\dot{\alpha} c}{V} + g_{AM,\beta}(x)\beta + g_{AM,camb}(x) + g_L(\ddot{y}, \ddot{\alpha}, \dot{\beta}, \ddot{\beta}, x) \quad (2)$$

It in the presentation of the expressions above, $\alpha_{C,eff}$ can be considered an effective three quarter angle of attack, and corresponds to the circulatory forces in [9]. In the terminology of that work it corresponds to *QC/V*. Please note that the circulatory forces include in addition to the common terms also the effect of the trailing edge flap deflection and it's time rate of change. For an excellent introduction to the concept of splitting forces into circulatory and non-circulatory forces please refer to the classic paper by Von Karman and Sears [18]. In terms of a time simulation, this effective three quarter chord angle can be considered a filtered version of the quasisteady value given below.

[1] The Kutta condition is in fact an enforcement of viscous effects at the trailing edge, preventing unphysical infinitely big gradients at the trailing edge. The Kutta condition is the only effect of viscosity taken into account in thin airfoil theory.

[2] The effect of omitting the influence from the x-degree of freedom was investigated in [15], where it was found that with regards to aeroelastic stability, this has negligible effect on the results. It is therefore assumed that this is also the case for the forces.

$$\alpha_{C,QS} = \alpha - \frac{\dot{y}}{V} + (1/2 - a)\frac{c}{2V}\dot{\alpha} - \alpha_0 - \frac{H_{dydx}}{2\pi}\beta - \frac{H_y}{2\pi}\dot{\beta} \quad (3)$$

The first line in the above is an effective flat plate three quarter angle of attack, and the lower line introduces the effect of the deformable trailing edge. The constants $H_{:}$ depend on the trailing edge deformation mode of the flap deflection. Please consult [9] for details on this. From potential flow theory the constant k_C has the value

$$k_C = 2\pi, \quad (4)$$

but can in general be interpreted as the steady lift curve slope. The term in Equation (1) involving the time rate of change of α is for wind turbine applications usually the biggest of the rest of the force terms, the so-called added-mass terms, and the associated constant has the value

$$k_{\dot{\alpha}} = \frac{\pi}{2} \quad (5)$$

The remaining added mass terms have been put into the linear function k_L. The magnitude of these terms will be addressed later.

For the terms in Equation (2), we see now that the pressure difference is of course dependent on the non-dimensional position, x, on the airfoil. In this work we use the nondimensional chordwise parameter, also used in [9], set to zero at the mid-chord and nondimensionalized with the half-chord, such that the values x=-1 and x=1 corresponds to the leading and trailing edge, respectively. It is seen that the circulatory pressure difference scale with the same parameter as the circulatory lift: $\alpha_{C,eff}$. Hence, by estimating this parameter from measurements of the pressure difference over the airfoil, the unsteady lift can be estimated. From [9] we have the functional form of the corresponding distribution of the pressure difference

$$g_C(x) = 4\frac{1-x}{\sqrt{1-x^2}} \quad (6)$$

This function can be determined from measurements or computations as the partial derivative of the pressure difference coefficient with respect to angle of attack under steady conditions.

From [9] we further get

$$g_{\dot{\alpha}}(x) = 4\sqrt{1-x^2} - \frac{1-x}{\sqrt{1-x^2}} \quad (7)$$

The shape of this is more difficult to estimate from computations or measurements because of the unsteady nature, so it is suggested to keep (7) also when other constants and functions are derived from computations or measurements.

The next term in (2) is the part of the pressure difference due to the deflection of the trailing edge that is not included in the circulatory terms. This part of the pressure difference has no "memory effect", and the corresponding integral lift from this is zero. The scaling function of this part can derived for the tin airfoil case from the results in [9]

$$g_{AM,\beta}(x) = \frac{2}{\pi}\left(\frac{\partial f_{dydx}(x)}{\partial x} - \frac{x}{\sqrt{1-x^2}}H_{dydx}\right) \quad (8)$$

Here the function f_{dydx} is defined from the trailing edge deformation shape, see [9] for details. Analogous to this term, the added mass term of the basic camber is

$$g_{AM,camb}(x) = \frac{2}{\pi}\left(\frac{\partial f_{dydx,camb}(x)}{\partial x} - \frac{x}{\sqrt{1-x^2}}2\pi\alpha_0\right) \quad (9)$$

This function can be determined from steady measurements or computations as the pressure difference coefficient for undeflected trailing edge at the angle where lift is zero, $\alpha=\alpha_0$. From this, the scaling function in Equation (8) may be derived for an actual airfoil, since that can be interpreted as

$$g_{AM,\beta}(x) = \frac{\Delta p_{st,\alpha=0,\beta=1}(x) - \Delta p_{st\alpha=0,\beta=0}(x)}{\frac{1}{2}\rho V^2} - g_C(x)\frac{\left(\frac{\partial C_l}{\partial \beta}\right)}{\left(\frac{\partial C_l}{\partial \alpha}\right)} \quad (10)$$

Since this term represents the difference between the steady circulatory distribution and the actual pressure difference due to a deflection of the trailing edge with the same total lift, we see that the point on the airfoil where (8) or alternatively (10) is zero represents the point where changes in pressure difference is directly proportional to changes in lift in the steady case. For most trailing edge deformation shapes this is fairly close to mid chord. This means that a control aiming at keeping the pressure difference in this chordwise point constant would result in a constant lift in the steady case.

As for the lift, the effect of the remaining terms on the pressure difference is put in the function g_L. A discussion on the relative magnitude of this is given later.

As hinted to earlier, the case where thickness is included the functions and constants in the linear expressions (1) and (2) may have slightly different values and shapes. A preliminary investigation of this was undertaken using a panel code described in [19]. The results showed that adding the geometric nonlinearities does not influence the conclusions from the linear thin airfoil theory considerably on the largest part of the chord. Only in a region very close to the leading edge are the linear behavior found in the nonlinear computations. So it is assumed that the linear functionality in (1) and (2) are also applicable in the case of non-zero thickness airfoils, where the constants and functions therefore may have slightly different values than the ones derived for the thin airfoil case in [9].

Therefore it is justified to further use the thin airfoil theory to derive a load reduction control based on the thin airfoil theory results. Further adding viscosity could influence results, but we will proceed with the assumption of the effects of that being expressible in the form of (1) and (2).

Under the assumption that the most important unsteady terms in (1) and (2) are the circulatory terms, the pith rate terms, the TE deformation angle term and the camber term we have a set of equations for determination of an approximate lift coefficient

$$C_{L,est} = \frac{L_{est}}{0.5\rho V^2 c} = k_C \alpha_{C,eff} + k_{\dot{\alpha}} \frac{\dot{\alpha} c}{V} \tag{11}$$

$$C_{\Delta p,est}(x) = g_C(x)\alpha_{C,eff} + g_{\dot{\alpha}}(x)\frac{\dot{\alpha} c}{V} + g_{AM,\beta}(x)\beta + g_{AM,camb}(x) \tag{12}$$

If we consider the case where two difference pressures are measured, we can set up a liner system for estimation of the effective circulatory angle and the pitch rate term from (12). For this we use also knowledge of the trailing edge deformation angle and the functions in (12) from thin airfoil theory or derived from measurements or computations.

$$\begin{bmatrix} \alpha_{C,eff} \\ \frac{\dot{\alpha} c}{V} \end{bmatrix} = \overline{A}^{-1} \begin{bmatrix} C_{\Delta p,est}(x_1) \\ C_{\Delta p,est}(x_2) \end{bmatrix} - \left(\overline{A}^{-1} \begin{bmatrix} g_{AM,\beta}(x_1) \\ g_{AM,\beta}(x_2) \end{bmatrix} \right) \beta - \left(\overline{A}^{-1} \begin{bmatrix} g_{AM,camb}(x_1) \\ g_{AM,camb}(x_2) \end{bmatrix} \right) \tag{13}$$

Where the **A** matrix is given by

$$\overline{A} = \begin{bmatrix} g_C(x_1) & g_{\dot{\alpha}}(x_1) \\ g_C(x_2) & g_{\dot{\alpha}}(x_2) \end{bmatrix} \tag{14}$$

This estimation of the two terms can now be input in Equation (11) to get an estimate for the unsteady lift on the airfoil including both terms. Investigation of the terms in (11), (13) and (14) further show that a choice of x_1=-3/4 and x_2=0, corresponding to difference pressure measuring stations at chordwise positions 12,5% and 50% from the leading edge.

A reduced and therefore less accurate estimation of the lift based on only one measurement point can be done by neglecting the influence of the alpha dot term (because this is generally the smaller term of the two). Rearranging (12) results in

$$\alpha_{C,eff} = \frac{C_{\Delta p,meas}(x) - g_{AM,\beta}(x)\beta - g_{AM,camb}(x)}{g_C(x)} - \frac{g_{\dot{\alpha}}(x)}{g_C(x)}\frac{\dot{\alpha} c}{V} \approx \frac{C_{\Delta p,meas}(x) - g_{AM,\beta}(x)\beta - g_{AM,camb}(x)}{g_C(x)} \tag{15}$$

Since the pressure difference corresponding to the alpha dot term would be interpreted as noise, it makes sense to measure the pressure in the point where the measurement is not influenced by that mode. From Equation (7) we see that this is in x=-3/4, corresponding to 12,5% of the chordlength from the leading edge.

After estimation of the circulatory term, we get the estimation of the lift coefficient by neglecting the alpha dot term in (11)

$$C_{L,est} = k_C \alpha_{C,eff} \quad (16)$$

Therefore the estimation of the lift coefficient may be summarized as below:

1 Δp estimation: Equations (15) and (16)

2 Δp estimation: Equations (11), (13) and (14)

An investigation of the performance of the two different methods using input obtained from the same setup as the AOA control in [8], and it was found that the RMS error on the estimated lift compared with the RMS on the full lift was 5.8% for the 1 Δp estimation case, and only 1.2% on the 2 Δp estimation case. This shows a very promising lift estimation capability.

2.2 Load reduction algorithms

Each of the two ways of estimating the unsteady lift was used to make a PI control seeking to keep the lift constant. Both controls were used in the same type of 2D aeroelastic setup (general 2D setup) as used in [8]. The readers are referred to the original reference for details on the aeroelastic setup.

Δp control

For both of the control algorithms using the pressure difference measurements the following simple PI control aiming at keeping the lift constant:

$$\beta = K_P (C_{L,est} - \overline{C}_{L,est}) \quad (17)$$

Note that the overbar signifies a running mean value.

For the sake of completeness, the other two controls originally propsed in [8], here used for reference, are outlined below.

AOA control

The “alpha” controller primarily reacts to changes in the incidence and relative velocity from a multi whole pitot tube mounted near the leading edge of the airfoil, furthermore, the “alpha” controller assumes the airfoil torsional deflections known.
The “alpha” controller is based on the following equations

$$\beta = \frac{\frac{\partial C_l}{\partial \alpha}}{\frac{\partial C_l}{\partial \beta}} \left(\tan^{-1}\left(\frac{V_\infty - \frac{\partial y}{\partial t}}{\omega r} \right) + \theta + (0.5 - a)b\frac{\frac{\partial \theta}{\partial t}}{V} - \alpha_0 \right) - \beta_0$$

$$\alpha_0 = \frac{1}{\tau}\int_{t-\tau}^{t} \alpha \, dt$$

$$\beta_0 = \frac{1}{\tau}\int_{t-\tau}^{t} \beta \, dt$$

, the time constant “τ” is used to determine the time window for the reference incidence “α0” and TE deflection angle “β0”. The rotational speed of the rotor is “ω”, and the radial position of the airfoil is “r”. The free wind speed is “V∞” and the relative wind speed seen by the airfoil is “V”. The unsteady torsional deflection of the airfoil is “θ”. The chord is “c”, the half chord is “b” and “a” is based on the elastic axis measured from the leading edge “l” as

$$a = \frac{2l}{c} - 1$$

Flap control

The flapwise deflection is assumed known for the “flap” controller supposedly using a series of strain gauges or optic fibers embedded in the blade.
The “flap” controller is based on the following equations, “Kp“ and “Kd” are gains and “y” indicates the flapwise deflection.

$$\beta = K_p(y - y_0) + K_d \frac{\partial y}{\partial t}$$

$$y_0 = \frac{1}{\tau}\int_{t-\tau}^{t} y \, dt$$

The time constant “τ” is used to determine the time window for the reference flapwise deflection or baseline “y0”. If the time constant is small low-frequency deflections will be ignored by the controller and visa versa. Gain tuning for the proportional and differential gain is described in [8]. For a more rigorous treatment, please refer to the original work.

3. Results

In order to evaluate the load reduction capability of the postulated trailing edge flap control methods simulations using the same 2D setup as in the original work of Buhl *et. al.* [8] was used. In order to evaluate the load reduction relative to the trailing edge flap control algorithm shown in that work, the same algorithms was implemented in the tool used for the present calculations.

2 Δp control

Much to the authors' surprise, the simple PI control employing the most accurate version of the estimation of the lift turned out to be aeroelastically unstable at even very low control gains. In fact, it was unstable to the point of not being usable for load reduction. The triggered instability mode was mostly a combination of the torsional mode and trailing edge flapping.

Following this finding, it was tested to run a simple PI control of the TE flap based on the exact lift force, and result of this was also an unsteady control. Again with the triggered unstable mode being a combination of the torsional mode and trailing edge flapping.

Based on this, it was concluded that in order to make an algorithm using a precise estimate of the lift force stable we will have to look into the coupling with the torsional degree of freedom, in which stability tools such as [14,15] can shed light on the mechanisms at play.

1 Δp control

Despite the very unstable behavior of the 2 Δp control, the one based on the slightly less accurate estimation of the unsteady lift showed good results. Figure 2 below show the load reduction as function of control gain for the 1Δp controller.

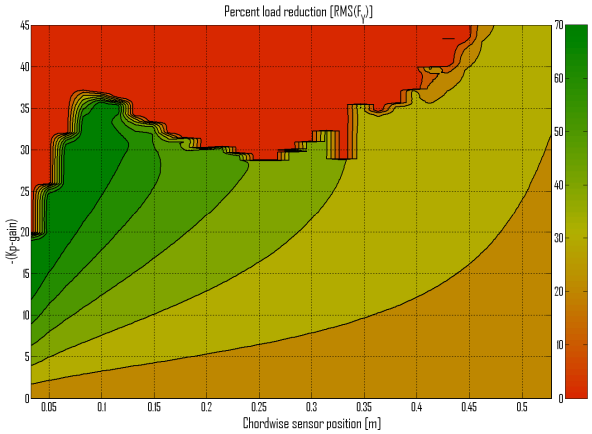

Figure 2; Load reduction as function of gains (Y-axis) and sensor position (X-axis).The default parameters are used for the 2D model.

As expected, the best load reduction potential, 74%, is obtained close to 12,5% from the leading edge. It is noted that the best load reduction potential occurs close to the region where the control gets unstable (red region). Further, it is noted that the load reduction potential close to mid-chord where the beta correction term vanishes, is rather poor.

Figure 3 show a comparison of the load reduction potential of the 1Δp load reduction algorithm against the two others originally shown in [8].

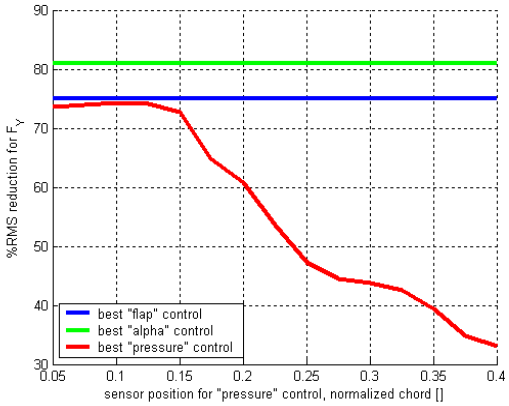

Figure 3; load reduction comparison between the original "flap" and "alpha" controller and the proposed simple "pressure" controller as a function of chordwise position of pressure sensor.

It is seen here, that the best load reduction from the 1Δp control is close to the load reduction capability of the flap control. The AOA control, however, is still somewhat higher. For the sake of making a fair comparison it should be stressed that the full AOA control includes the knowledge of the pitch rate. This is, however, probably very hard to measure on a wind turbine, so, the green curve may be unrealistically high whereas the 1Δp control does not use input data that are hard to measure on a real turbine.

Results from investigations of the influence of section weight are shown in Figure 4 below.

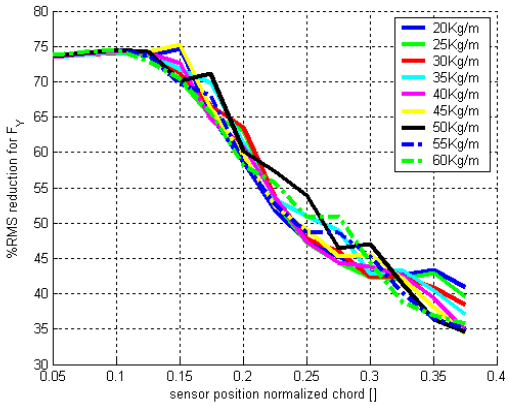

Figure 4; Flapwise load reduction as a function of overall cross sectional weight and chordwise position of pressure sensor

It is seen that the cross sectional weight does not influence load reduction capability much. Figure 5 below shows load reduction for different positions of the centre of gravity.

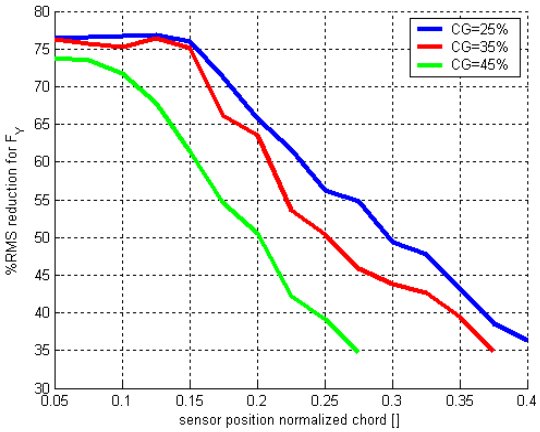

Figure 5; Flapwise load reduction as a function of chordwise position of center of gravity and chordwise position of pressure sensor

It is observed that the best location of the pressure difference measurement point is close to 12.5% from the leading edge, confirming the speculations in section 2.1 on the disturbing effect of the alpha dot term.

A series of additional simulations have been made for the "pressure" controller which adds signal noise and time delay in the control signal. The time delay is implemented as a simple stack which delays the control signal in 5,10,15 … 40, 45 milliseconds. The signal noise is implemented as a Gaussian random distribution where the standard deviation is 1,2,3... 8,9% of the full scale sensor range. The proportional gain can, as for the results shown in Figures 3 to 5 be readily found using a simple one parameter local optimum search. The results from the investigations are shown in Figures 6 and 7.

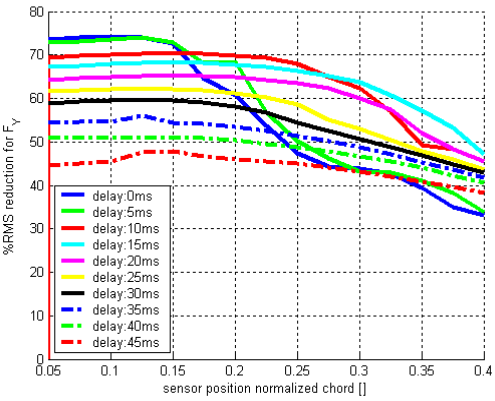

Figure 6; Flapwise load reduction as a function of delay in sensor signal and chordwise position of pressure sensor

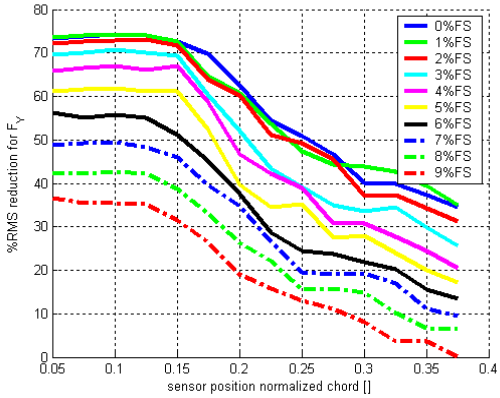

Figure 7; Flapwise load reduction as function of introduced error in signal and chordwise position of pressure sensor

For both the time delay and introduced error cases it is seen that the best placement for the sensor in the 1Δp algorithm is close to 12.5% from the leading edge regardless of time delay or introduced random error. In agreement with earlier studies using the AOA and flap controls [8], it is seen in Figure 6, that time delay has a strong deteriorating effect on the load reduction potential. The same trend is seen for the random error case in Figure 7.

It should be mentioned that a preliminary study of the load reduction capabilities of AOA and 1Δp algorithms was investigated using CFD [17]. Although not testing more than one chordwise location of the pressure difference measurement, probably not fine tuning the constants in the control algorithm, both algorithms showed a very good and almost equally big load reduction potential.

4. Conclusions and further work

Encouraged by the strong link between the pressure differences over an airfoil and the integral lift in combination with the belief that measurement of such pressure differences on a real turbine would be easier, cheaper and more robust than a pitot-tube based estimation of the lift spurred the investigations in the present paper on using measurements of the pressure difference over an airfoil to control a TE flap for smart rotor fatigue load reduction.

Based on the theoretical 2D unsteady thin airfoil response of the lift and pressure difference over an airfoil two algorithms/methods were postulated for estimating the unsteady lift on an airfoil section from measurements of the pressure difference over the airfoil pressure and suction side: One algorithm employing measurement of

the pressure difference at one chordwise location, and another algorithm using measurement of the pressure difference at two different chordwise locations.

Analysis of the response from unsteady simulations using a 2D thin-airfoil potential flow algorithm coupled with a model for the structural response and a turbulent wind input concluded that it is possible to estimate very accurately the unsteady lift of an airfoil section with a TE flap using pressure difference measurements.

Encouraged by this, a simple PI control algorithm was formulated, with the aim of keeping the estimated lift constant. The simple one pressure difference based control algorithm turned out to have a good load reduction potential, and the best load reduction potential was obtained when using a difference pressure measured close to 12,5% from the leading edge. This result indicates that the disturbing factor is the added mass term including the time derivative of the torsion.

The second pressure difference measurement based algorithm, based on the more accurate estimation of unsteady lift from two pressure difference measurements, turned out to cause an aeroservoelastic instability (torsion-TE flap) which hindered any load reduction potential.

An initial investigation of the unstable behavior was undertaken, where the conclusion was that if the exact lift is used as an input to a simple PI regulator seeking to maintain a constant lift, the result is an aeroservoelastically unstable system. The unstable mode mainly involved the torsional and the TE flap action. Further analysis of the mechanisms in play is needed to pinpoint the mechanisms responsible for the instability. This might make possible new, more effective, TE flap control algorithms employing pressure difference measurements in more than one chordwise position.

In conclusion it should be mentioned that even though the AOA control algorithm yielded a higher load reduction potential, practical implementation of that exact algorithm on real turbines may result in lower load reductions, since it is here assumed that the torsional velocity is known to the control algoritnm. This may be hard to get on a real turbine. Further study of the effect of not knowing this in the AOA control is recommended to compare the control algorithms on a fair basis.

Acknowledgements

The authors gratefully acknowledge that a part of the financial support for this work was obtained from the Advanced Technology Foundation in Denmark.

References

[1] Larsen, T.J., Madsen, H.Aa. and Thomsen, K. "*Active Load Reduction Using Individual Pitch, Based on Local Blade Flow Measurements*", Wind Energy, Vol. 8 issue 1, p. 67-80, 2004

[2] Bossanyi, E.A., "*Developments in Individual Blade Pitch Control*", Wind Energy, Vol. 6 issue 3, p. 229-244, 2003

[3] Barlas, T. and G.A.M. van Kuik, "*State of the art and prospectives of smart rotor control for wind turbines*". In Journal of Physics 5, 2007 "2nd EWEA, EAWE The Science of making Torque from Wind conference at DTU, 28-31 August 2007".

[4] Van Dam, C.P., R. Chow, J.R. Zayas and D.A. Berg, "*Computational investigations of small deploying tabs and flaps for aerodynamic load control*". In [Technical paper] Journal of Physics 5, 2007 "2nd EWEA, EAWE The Science of making Torque from Wind conference at DTU, 28-31 August 2007".

[5] Andersen P.B., Gaunaa M., Bak C., Hansen M.H., "*A Dynamic Stall Model for Airfoils with Deformable Trailing Edges*", Journal of Physics 5, 2007 "2nd EWEA,EAWE The Science of making Torque from Wind conference at DTU, 28-31 August 2007

[6] Basualdo, S., "*Load alleviation on wind turbine blades using variable airfoil geometry*", Wind Engineering, vol. 29, no. 2, 2005

[7] Troldborg, N., "*Computational study of the Risø-B1-18 airfoil with a hinged flap providing variable trailing edge geometry*", Wind Engineering, vol. 29, no. 2, 2005

[8] Buhl, T.; Gaunaa, M.; Bak, C.; "*Potential Load Reduction Using Airfoils with Variable Trailing Edge Geometry*"; Journal of Solar Energy Engineering; November 2005, Vol. 127, p. 503-516

[9] Gaunaa, M., "*The Unsteady 2D Potential-Flow Forces on a Variable Geometry Airfoil Undergoing Arbitrary Motion*", Risø-R-1478, 2006

[10] Andersen, P.B.; Henriksen, L.C.; Gaunaa, M.; Bak, C.; Buhl, T., "*Integrating deformable trailing edge geometry in modern Mega-Watt wind turbine controllers"*. In: Scientific proceedings. 2008 European Wind Energy Conference, Brussels

[11] Abdallah, I.; "*Advanced Load Alleviation for Wind Turbines using Adaptive Trailing Edge Geometry: Sensoring Techniques.*" M.Sc Thesis Project; July 13, 2006, Technical University of Denmark, Department of Mechanical Engineering, Section of Fluid Mechanics

[12] Bak, C.; Gaunaa, M.; Andersen, P.B.; Buhl, T.; Hansen, P.; Clemmensen, K.; Møller, R., "*Wind tunnel test on wind turbine airfoil with adaptive trailing edge geometry*." In: [Technical papers] presented at the 42. AIAA aerospace sciences meeting and exhibit. 45. AIAA aerospace sciences meeting and exhibit, Reno, NV (US), 8-11 Jan 2007. (American Institute of Aeronautics and Astronautics, Reston, VA, 2007) (AIAA-2007-1016)

[13] Buhl, T., Gaunaa, M. & Andersen, P.B., "Stability limits for a full wind turbine equipped with trailing edge systems", Conference paper for EWEC 2009, Marseilles.

[14] Gaunaa, M. "*Investigation of the Effect of Deformable Trailing Edge Geometry Control Systems on Flutter Velocity*", Paper and Poster at EWEC 2006, Athens.

[15] Bergami, L., Gaunaa, M. and Hartvig, M. H. Hansen "*Investigation of Stability Issues for an Adaptive Trailing Edge System"* Paper and Presentation at AIAA-2009 Orlando, USA. Jan 2009.

[16] Larsen T.J., Hansen A.M. "*Influence of Blade Pitch Loads by Large Blade Deflections and Pitch Actuator Dynamics Using the New Aeroelastic Code HAWC2*", paper and oral presentation at EWEC 2006, Athens.

[17] Heinz, J. "*Investigation of Piezoelectric Flaps for Load Alleviation Using CFD*". Master Thesis, Risø DTU, November 2008.

[18] von Karman, Th. & Sears,W.R. *"Airfoil Theory for Non-Uniform Motion"*. Journal of the Aeronautical Sciences. 5(10) 1938. p.379-390.

[19] Gaunaa, M. "*Unsteady Aerodynamic Forces on a NACA 0015 Airfoil in Harmonic Translatory Motion*". PhD Thesis, DTU, Denmark, April 2002.